IEEE Open Journal of the Communications Society

Received XX Month, XXXX; revised XX Month, XXXX; accepted XX Month, XXXX; Date of publication XX Month, XXXX; date of current version 11 January, 2024.

Digital Object Identifier 10.1109/OJCOMS.2024.011100

A Polar-Coded PAPR Reduction Scheme Based On Hybrid Index Modulation

Si-Yu Zhang[1,2] *(Member, IEEE)*, Xinwei Yue[2] *(Senior Member, IEEE)*, Behnam Shahrrava [3] *(Member, IEEE)*, Yuexia Zhang[1,2] *(Senior Member, IEEE)*, AND Gongpu Wang[4] *(Member, IEEE)*.

[1]Key Laboratory of Information and Communication Systems, Ministry of Information Industry, Beijing Information Science and Technology University, Beijing, China
[2]Key Laboratory of Modern Measurement and Control Technology, Ministry of Education, and School of Information and Communication Engineering, Beijing Information Science and Technology University, Beijing, China
[3]Department of Electrical and Computer Engineering, University of Windsor, Ontario, Canada
[4]Beijing Key Lab of Transportation Data Analysis and Mining, School of Computer and Information Technology, Beijing Jiaotong University, Beijing, China

CORRESPONDING AUTHOR: Si-Yu Zhang (e-mail: zhang1fs@bistu.edu.cn).

This work was supported in part by the National Natural Science Foundation of China (NSFC) under Grant 62301058, and R&D Program of Beijing Municipal Education Commission under Grant KM202411232010

ABSTRACT

Orthogonal frequency division multiplexing with index modulation (OFDM-IM) is a promising technique for next-generation wireless communications due to its superior error performance and flexibility. However, as a type of multi-carrier modulation, it suffers from a high peak-to-average power ratio (PAPR), which can compromise transmission reliability. Therefore, in this paper, a polar-coded PAPR reduction scheme based on hybrid index modulation (PC-HIM) for OFDM-IM is proposed. Also, the proposed framework employs sets of various frozen bits and spatial modulation (SM) to solve the high PAPR issue in OFDM-IM systems. At the receiving side, the detection of the activated antennas status facilitate the recovery of selected frozen bit set, whose indices are embedded in the SM operations. Therefore, the need for transmitting side information, which is a necessary process in probabilistic PAPR reduction schemes, can be eliminated. Further, to enhance detection accuracy, a construction method for frozen bit sets based on Hadamard matrix is proposed. Additionally, to address the high complexity inherent in the proposed PC-HIM PAPR reduction framework, a low-complexity version, termed LC-PC-HIM, is proposed. This framework simplifies both the transmitting and receiving operations through a redesign of the information processing procedures and the selected frozen bit set detection step. Simulation results demonstrate that the proposed PAPR reduction scheme (PC-HIM and LC-PC-HIM) outperforms existing polar code-based PAPR reduction schemes by at most 12.5%, delivering the most effective PAPR reduction performance. Furthermore, the proposed receiving approach achieves error performance comparable to that of a receiver utilizing perfect side information.

INDEX TERMS Polar code; Orthogonal frequency division multiplexing (OFDM); Index modulation (IM); Peak-to-average power ratio (PAPR); Spatial modulation (SM); Side information.

I. INTRODUCTION

Orthogonal frequency division multiplexing (OFDM) has been extensively adopted in 4G/5G and optical communication systems due to its high data rate, exceptional spectral efficiency, and robustness against multi-path interference [1]. To augment the robustness and adaptability of OFDM, the concept of OFDM with index modulation (OFDM-IM) was introduced in work [2]. As an innovative technique for next-generation communication systems, OFDM-IM incorporates spatial modulation (SM) into the

frequency domain, enhancing the system architecture [3]–[5]. The flexible structure of OFDM-IM provides good trade-off between energy efficiency and spectral efficiency. Furthermore, it has been demonstrated that the inactive sub-carriers in OFDM-IM significantly bolster its resistance to inter-carrier interference (ICI), making it particularly suitable for applications in vehicular [6], [7] and high-speed railway (HSR) communications [8]. Also, many potential technologies for 6G, such as non-orthogonal multiple access (NOMA) and orthogonal time frequency space (OTFS), can be combined with IM, which provides a promising chance for IM to be applied in the next generation communications systems [9]–[11].

As forms of multi-carrier modulation, both OFDM-IM and traditional OFDM share a critical limitation: a high peak-to-average power ratio (PAPR). This issue arises from the coherent summation of symbols transmitted across various sub-carriers, inherent to the structure of multi-carrier signals [12]. High PAPR can induce in-band and out-of-band distortion when signals are amplified by high power amplifiers (HPAs). Without effective PAPR reduction techniques, OFDM-based signals could lead to substantial power inefficiencies at the transmitter, posing significant challenges for battery-operated wireless devices. Moreover, high PAPR in OFDM-IM signals may result in nonlinear distortions and degrade system performance [13]. As next-generation communication technologies transition from centimeter waves to millimeter waves [14], addressing the high PAPR issue becomes increasingly crucial, particularly given that HPAs are major contributors to energy consumption in cellular networks [15].

The issue of high PAPR has been extensively studied and comprehensively reviewed in the literature, particularly in references [16] and [17]. Among the existing PAPR reduction techniques, clipping and companding schemes have demonstrated effectiveness in reducing the PAPR to acceptable levels. However, these approaches introduce significant signal distortion, requiring compensatory methods at the receiving end. Conversely, probabilistic techniques such as selective mapping (SLM) [18] and partial transmit sequence (PTS) [19] offer substantial PAPR reduction without compromising signal integrity. However, such schemes need transmit side information to the receiver for signal recovery. This operation compromises the transmission data rate and increase the complexity [20]. In 6G systems with massive multiple input multiple output (MIMO), hundreds of antennas sending side information will cause side information burden [21]. While most established PAPR reduction schemes are readily adaptable to OFDM-IM, the development of efficient PAPR reduction methods that capitalize on the unique structure of OFDM-IM remains a challenging area of research. Recent studies have explored the potential of idle sub-carriers for PAPR reduction in OFDM-IM through the introduction of dither signals, as discussed in [22], [23], and [24]. These schemes successfully mitigate PAPR but at the expense of the system's error performance, highlighting the trade-offs involved in these approaches.

Polar codes represent a significant advancement in channel coding and information theory due to their simplicity in encoding and decoding processes. These codes have been adopted for the channel coding of enhanced mobile broadband (eMBB) control channels in the 5G new radio (NR) interface, as discussed in [25]. Research indicated in [26] has demonstrated that polar-coded OFDM-IM exhibits superior error performance compared to conventional OFDM systems. Fortuitously, by making use of the frozen bits inherent to polar codes and the idle structure of OFDM-IM, the PAPR of multi-carrier modulation can be effectively managed. Reference [27] introduces an innovative polar-coded PAPR reduction scheme, which inserts PAPR reduction bits at the locations of frozen bits. However, the limited number of available PAPR reduction bits restricts the effectiveness of this approach, also impacting the error performance adversely. Further developments include the implementation of polar-coded OFDM-IM SLM and PTS schemes, as proposed in [28] and [29], respectively. These schemes reduce the PAPR by utilizing randomly selected frozen bits and interleaved idle sub-carriers, which are determined by the frozen bits. Nonetheless, to eliminate the need for transmitting side information, both approaches employ multiple polar decoders, thereby significantly increasing the overall system complexity. In [13], it has been demonstrated that the use of random frozen bits introduces an interleaving-like effect due to index modulation, which significantly enhances the system's PAPR reduction performance compared to similar schemes without interleaving. Furthermore, related research on polar codes-based PAPR reduction techniques is discussed in [30]–[32]. These studies incorporate polar codes into various traditional PAPR reduction methods, such as SLM and chaotic sequences, achieving notable PAPR reduction. However, these approaches do not account for the unique structure of IM. Additionally, as these PAPR reduction schemes rely on probabilistic techniques, they inherently suffer from high computational complexity, which remains a significant challenge.

In this paper, we propose a novel polar-coded PAPR reduction scheme employing hybrid index modulation (PC-HIM), aimed at enhancing PAPR reduction performance in OFDM-IM systems while simultaneously achieving a low-complexity side information free scheme at the receiver. The PC-HIM leverages a set of randomly selected frozen bits to adopt a SLM-like approach for PAPR reduction. Additionally, spatial modulation (SM) [33] is also employed within the framework to further augment both PAPR reduction and error performance. The index bits for SM are selected based on the frozen bit set that yields the lowest PAPR, facilitating simplified detection at the receiver through active antenna identification, thus circumventing complex polar decoding procedures in [28] and [29]. To further address complexities in transmission and reception, we introduce

a low-complexity PC-HIM (LC-PC-HIM) that reduces the number of inverse fast Fourier transform (IFFT) operations required at the transmitter and shortens the length of detected frozen bits at the receiver. Furthermore, the proposed (LC-PC-HIM) incorporates a method for constructing frozen bit sets using Hadamard matrix to enhance detection accuracy.

Simulation results confirm that the proposed (LC-PC-HIM) scheme outperforms existing polar code-based PAPR reduction techniques in terms of PAPR reduction performance. Additionally, it achieves error performance comparable to the ideal reception scenario, with significantly reduced complexity relative to the existing polar-coded PAPR reduction schemes. The contribution of this paper can be summarized as follows:

- In this paper, a novel polar-coded PAPR reduction framework that incorporates both frequency and spatial index modulation for OFDM-IM systems is proposed. At the transmitter, the proposed PC-HIM framework employs hybrid IM to significantly enhance PAPR reduction performance. At the receiver, the implementation of SM demodulation allows for accurate identification of the selected frozen bit set, achieving this with reduced complexity.
- To mitigate the computational complexity associated with the PC-HIM, we propose a LC-PC-HIM framework. On the transmitting side, the LC-PC-HIM approach involves selecting the candidate sequence exhibiting the lowest PAPR prior to SM, thereby significantly simplifying the computational demands. On the receiving side, complexity reduction is further achieved by limiting the frozen bit set detection to a partial length of the frozen bits, streamlining the overall receiving process.
- To further enhance the accuracy of frozen bit set selection, a Hadamard-based frozen bit sets construction method is proposed. This method allows the receiver to improve the detection performance of frozen bit sets using shorter sequences of detected frozen bits. This approach utilizes the properties of Hadamard codes to optimize the identification process, thereby facilitating low complexity and accurate receiving.

The structure of this paper is organized as follows: Section II describes the system model used in the proposed PC-HIM scheme, which includes both OFDM-IM and polar codes. Section III details the proposed PC-HIM scheme, delineating the methodologies employed at both the transmitter and receiver, and also includes an analysis of the system complexity. Section IV presents the simulation results and evaluates the performance of the proposed PAPR reduction scheme. Finally, conclusions are drawn in Section V.

II. System Model

A. OFDM with Index Modulation

OFDM-IM systems represent a novel approach to frequency domain modulation using multiple sub-carriers. A distinguishing feature of OFDM-IM compared to traditional OFDM is that information bits are conveyed not only through the conventional modulation of sub-carriers but also through the activation status of these sub-carriers. Specifically, in OFDM-IM, certain sub-carriers may be intentionally set to zero, thus contributing to energy savings by reducing transmission power where possible. This technique allows for a balance between energy efficiency and spectral efficiency, which can be trade-off by adjusting parameters such as the number of sub-blocks, the number of sub-carriers per block, and the number of active sub-carriers within the overall system. Fig.1 depicts the OFDM-IM transmitter model, illustrating these concepts.

In an OFDM-IM system, the transmission process involves distributing m transmitted bits across G groups, with each group accommodating p bits. Concurrently, each OFDM block, having $\mathscr{N}_\ell$ sub-carriers, is segmented into G sub-blocks, each comprising n available sub-carriers. Within each sub-block g, a subset of k sub-carriers from n available ones is selected to be activated by symbols. Consequently, the relationship between the total bits and the structure of the OFDM block is established as $m = pG$ and $\mathscr{N}_\ell = nG$. The p bits assigned to each sub-block are further categorized into two subsets: p_1 and p_2, such that $p = p_1 + p_2$. The assignments of p_1 and p_2 bits are defined as follows:

$$\begin{aligned} p_1 &= \left\lfloor \log_2 \binom{n}{k} \right\rfloor, \\ p_2 &= k\log_2 \mathrm{M}, \end{aligned} \tag{1}$$

where $\lfloor \cdot \rfloor$ is the floor operation, $\binom{a_1}{a_2}$ represents the binomial coefficient and M is the constellation size.

For OFDM-IM, the block creation is not only performed by constellation mapping, but also by the indices of sub-carriers. Specifically, the indices of k active sub-carriers within each sub-block are determined by the initial p_1 bits, thereby facilitating the transmission of extra information. The indices indicating the k active sub-carriers in the g^{th} sub-block is written as:

$$\mathbf{I}_g = \{i_{g,1}, i_{g,2}, ..., i_{g,k}\}, \tag{2}$$

where $i \in \{1, \cdots, n\}$.

An illustrative example of index selection within a sub-block of an OFDM-IM system is presented in Table 1. Consider a sub-block configuration where $p_1 = 2$, $n = 4$, and $k = 2$. Take the first sub-block as an example, the index bits of length p_1 can assume any of four possible configurations: $[0, 0]$, $[0, 1]$, $[1, 0]$, or $[1, 1]$. These two index bits designate the positions of the active sub-carriers i. In the case of a sub-block with four sub-carriers, where only two are activated, there exist four potential combinations of

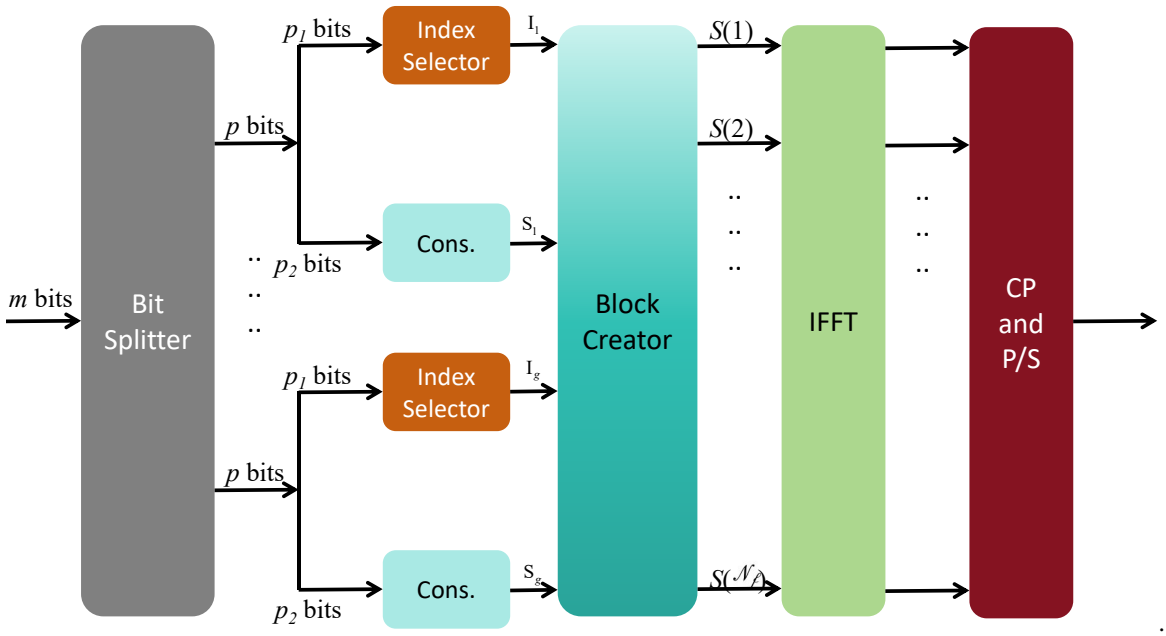

FIGURE 1. **The system model of an OFDM-IM transmitter**

active sub-carriers: $\mathbf{I}_{g_1} = [1, 2]$, $\mathbf{I}_{g_2} = [1, 3]$, $\mathbf{I}_{g_3} = [2, 4]$, and $\mathbf{I}_{g_4} = [3, 4]$. Sub-carriers that are not activated do not transmit any data and are typically set to a value of zero.

TABLE 1. **A Look-Up Table of Index Modulation for k = 4, and n = 2.**

Index Bits	Indices	Sub-blocks
[0, 0]	[1, 2]	[$S_g(1)$,$S_g(2)$,0,0]
[0, 1]	[1, 3]	[$S_g(1)$,0,$S_g(2)$,0]
[1, 0]	[2, 4]	[0,$S_g(1)$,0,$S_g(2)$]
[1, 1]	[3, 4]	[0,0,$S_g(1)$,$S_g(2)$]

After index modulation based on the first p_1 bits, the g^{th} OFDM sub-block can be denoted as:

$$\mathbf{S}_g = \begin{cases} S_g(\eta), & \eta \in \mathbf{I}_g \\ 0, & \text{otherwise}, \end{cases} \tag{3}$$

where $S_g(\eta)$ is obtained from a constellation Θ, and $\eta = 1, ..., k$. After concatenating all G sub-blocks, the OFDM block $\mathbf{S}$ is transformed to time domain through an IFFT operation. The spectral efficiency of OFDM-IM can be written as:

$$SE = \frac{(p_1 + p_2)}{n} = \frac{G(\lfloor \log_2 \binom{n}{k} \rfloor + k \log_2 \mathrm{M})}{\mathcal{N}_f}. \tag{4}$$

At the receiver, after the removal of cyclic prefix (CP), a fast Fourier transform (FFT) operation needs to be implemented. The OFDM-IM receiver needs to detect both the indices of active sub-carriers and the corresponding data symbols. For each sub-block g, the maximum likelihood (ML) detector can be applied by considering a joint detection for the indices of active sub-carriers and the carried on symbols:

$$\{\hat{S}_g(\eta)\}_{\eta=1}^{n} = \underset{\{S_g(\eta)\}_{\eta=1}^{n}}{\operatorname{argmin}} \sum_{\eta=1}^{n} |y_g(\eta) - h_g(\eta) S_g(\eta)|^2, \tag{5}$$

where $y_g(\eta)$ and $h_g(\eta)$ denote the received signal and channel frequency response on the η^{th} sub-carrier in the g^{th} sub-block. The searching space of the ML detection per bit is given by the order of $\mathcal{O}(\binom{n}{k} + \mathrm{M}^k)$ [34].

B. Polar Code

The introduction of Polar codes, as proposed by Arıkan in 2009 [35], represents a significant advancement in the field of information theory and has since garnered extensive research attention. Notably, polar codes have been integrated into the 5G communication standards by 3GPP [36], underscoring their importance and potential for future telecommunications frameworks, including 6G systems [37]. These codes are particularly valued for their low encoding/decoding complexity and their proven ability to achieve channel capacity. In this present section, the concept of the polar code is briefly introduced.

A construction of polar code with code length $\mathcal{N}_p$ and information length $\mathcal{K}_p$ is presented as an example. Here, a length-$\mathcal{K}_p$ information bits is denoted as:

$$\mathbf{u}_\mathrm{p} = ([u[1], u[2], ..., u[\mathcal{K}_p]), \tag{6}$$

and a length-N_p polar codeword is denoted as:

$$\mathbf{X}_\mathrm{p} = (X[1], X[2], ..., X[\mathcal{N}_p]), \tag{7}$$

respectively.

The construction of polar codes involves selecting $\mathcal{K}_p$ reliable sub-channels, referred to as bit positions, for the

transmission of information bits. These reliable positions are identified using various polar encoding schemes, such as the Bhattacharyya parameters [35] or the Gaussian Approximation (GA) [38]. In the terminology associated with polar encoding, bits placed in these reliable positions are termed as "free bits", and the set of indices containing these free bits is denoted by A. Conversely, the $\mathscr{N}_p - \mathscr{K}_p$ less reliable positions are designated for "frozen bits", denoted by $\mathbf{F}$, whose values and positions are predetermined and known to both the transmitter and receiver. The set of indices for these frozen bits is represented as A^c. Information bits are then transformed into codewords through the product with a generation matrix, $\mathrm{G}_2^{\otimes n}$. We denote this generation matrix, $\mathrm{G}_2^{\otimes n}$, as follows:

$$\mathrm{G}_2 = \begin{bmatrix} 1 & 0 \\ 1 & 1 \end{bmatrix}, \tag{8}$$

as the polar code kernel matrix. $\mathrm{G}_2^{\otimes n_p}$ indicates the $n_p{}^{th}$ Kronecker product of G_2, where $n_p = \log_2^{\mathscr{N}_p}$. A polar codeword $\mathbf{X}$ can be obtained by a matrix product:

$$\mathbf{X} = \mathbf{u}\mathrm{G}_{2,A}^{\otimes n_p} \oplus \mathbf{F}\mathrm{G}_{2,A^c}^{\otimes n_p}, \tag{9}$$

where $\mathrm{G}_{2,A}^{\otimes n_p}$ denotes the sub-matrix of $\mathrm{G}_2^{\otimes n_p}$ formed by the rows with the indices in A and so does $\mathrm{G}_{2,A^c}^{\otimes n_p}$. "$\oplus$" denotes the mod 2 operation. We note that if the frozen bits $\mathbf{F}$ are all zero, denoting as: $\mathbf{F}_0$, the generation process can be simplified to:

$$\mathbf{X} = \mathbf{u}\mathrm{G}_{2,A}^{\otimes n_p} \oplus \mathbf{F}_0\mathrm{G}_{2,A^c}^{\otimes n_p} = \mathbf{u}\mathrm{G}_{2,A}^{\otimes n_p}. \tag{10}$$

Polar decoding mechanisms have demonstrated that polar codes can asymptotically achieve channel capacity using successive cancellation (SC) decoding, provided that the code length is sufficiently long [35]. Additionally, polar codes are versatile in that they can accommodate variable code rates, decoding complexities, and error correction capabilities by employing different decoding algorithms. For instance, sphere decoding has been applied to enhance error correction performance in polar codes, although it entails a significantly high complexity [39]. Conversely, to maintain lower latency in polar decoding, belief propagation (BP) can be employed, despite potentially yielding sub-optimal performance compared to SC-based decoding [40], [41].

III. The Proposed Polar-Coded PAPR Reduction Scheme based on Hybrid Index Modulation

The proposed polar-coded PAPR reduction scheme, designated as polar-coded PAPR reduction scheme based on hybrid index modulation (PC-HIM), employs different sets of frozen bit and SM to jointly reduce PAPR. At the receiving end, the active antennas are detected, enabling the estimation of the utilized set of PAPR-reducing frozen bits. This approach facilitates PAPR reduction without the need for transmitting side information. Additionally, the integration of SM also enhances error and PAPR reduction performance. Moreover, to reduce the high complexity of the PC-HIM scheme, a low-complexity LC-PC-HIM framework is also introduced in this section. The LC-PC-HIM redesigns the PAPR reduction and frozen bit sets detection procedures of PC-HIM, resulting in a reduction of complexity. This section elaborates on the models for both the transmitting and receiving sides of the proposed PC-HIM and LC-PC-HIM PAPR reduction frameworks.

A. The Transmitter

Fig 2 provides an illustration of the proposed PC-HIM transmitting framework for PAPR reduction. This methodology employs an approach utilizing frozen bit sets, OFDM-IM, and SM to jointly reduce PAPR and facilitate accurate information reception. In the PC-HIM scheme, low PAPR signals are generated through the strategic use of random frozen bit sets combined with frequency-based IM. Additionally, this paper introduces enhancements to the PAPR reduction scheme by incorporating SM and a reception method to obviate the need for side information, thereby augmenting PAPR reduction capabilities without compromising error performance and transmission efficiency.

For an information sequence $\mathbf{U}$, as illustrated in Fig. 2, at first, a general polar codeword $\mathbf{X}_0$ is generated through:

$$\mathbf{X}_0 = \mathbf{U}\mathrm{G}_{2,A}^{\otimes n}. \tag{11}$$

To reduce PAPR, the proposed PC-HIM framework utilizes V sets of frozen bits $\mathbf{F}_v$, which are expressed as:

$$\mathbf{F}_v = (F_v[1], F_v[2], ..., F_v[\mathscr{N}_{fr}]), \tag{12}$$

where $v = 1, ..., V$. $\mathscr{N}_{fr}$ is the length of frozen bits. The frozen bits in $\mathbf{F}_v$ are selected from $\{0, 1\}$. The selection of frozen bits can be random or specific design in order to achieve better PAPR reduction and error performance. By utilizing V different frozen bit sets, V different codeword containing the same information can be obtained, which can be written as:

$$\mathbf{X}_v = \mathbf{X}_0 \oplus \mathbf{F}_v\mathrm{G}_{2,A^c}^{\otimes n} = \mathbf{X}_0 \oplus \mathbf{P}_v, \tag{13}$$

where $\mathbf{P}_v$ can be regarded as the phase rotation factors of the conventional SLM PAPR reduction scheme [18].

Fig.3 illustrates the generation of two distinct vectors using different sets of frozen bit. In the example depicted, an information sequence $[0, 1]$ is encoded using two 2-bit frozen bit sets, designated as $[0, 0]$ and $[1, 1]$, respectively. Through polar encoding and exclusive OR ($\oplus$) operations, two distinct polar codewords containing the same information are produced: $[1, 1, 1, 1]$ and $[0, 0, 1, 1]$. Subsequent index modulation and binary phase shift keying (BPSK) transform these into two OFDM-IM sub-blocks. Utilizing the mapping defined in Table 1, the resulting sequences post-frequency-domain IM are $[0, 0, -1, -1]$ and $[-1, -1, 0, 0]$, respectively. This approach, employing random frozen bit

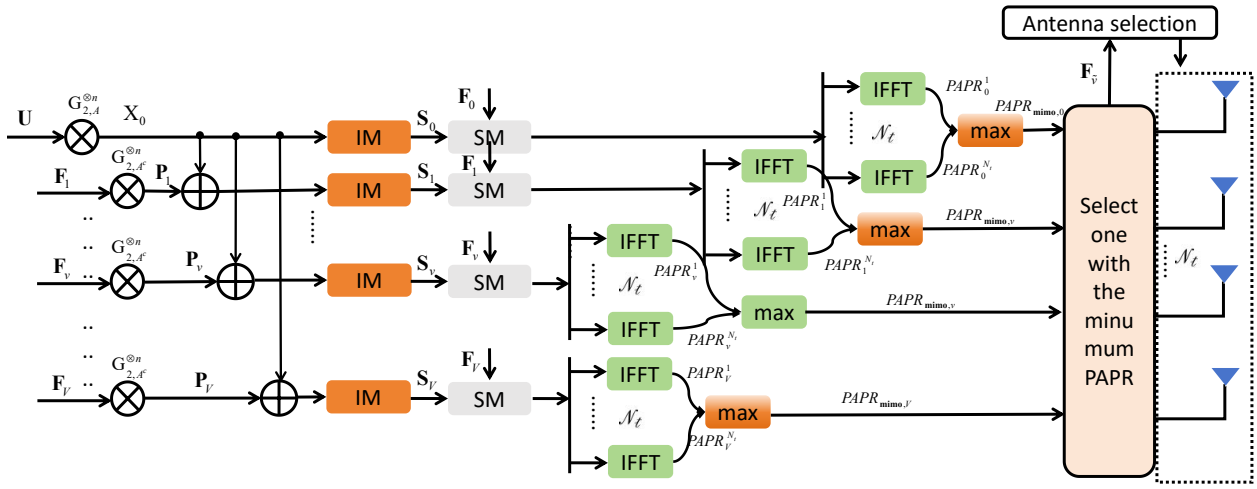

FIGURE 2. **The diagram of the proposed PC-HIM transmitting framework**

sets and index modulation, results in each candidate having a different PAPR. Additionally, by making use of the frequency domain IM, the proposed framework enables the candidate sequences to achieve a combined PAPR reduction performance enhancement from phase rotation and interleaving, which is demonstrated to be superior to employing only the phase rotation base PAPR reduction schemes [13].

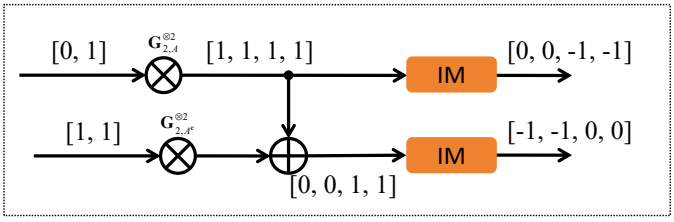

FIGURE 3. **An example of the candidates generation utilizing random frozen bit sets and index modulation**

It should be noted that a polar codeword generated exclusively with all zero-valued frozen bits can be denoted as $\mathbf{X}_0$. Following the generation of codewords using V distinct sets of random frozen bits, a total of $V+1$ codewords can be formed, each subject to a uniqie IM pattern. Subsequent to this, SM techniques are applied to each sequence of index-modulated symbols. In the SM mapping process, each candidate $\mathbf{S}_v$ is transformed to a $\mathcal{N}_t \times \mathcal{N}_\ell$ matrix $\mathbf{B}_v$, configured such that there is one nonzero element in each column, representing the position of an activated transmit antenna, while all other elements in the column are set to zero.

The SM procedure is a kind of index modulation in space domain. In the proposed PAPR reduction framework, the antenna selection is according to the different V sets of frozen bits in a sub-block g. The v^{th} frozen bits of $\mathbf{F}_v$ in sub-block g can be written as:

$$\mathbf{F}_{v,g} = (F_{v,g}[1], F_{v,g}[2], ..., F_{v,g}[n_{fr}]), \tag{14}$$

where $n_{fr} = \mathcal{N}_{fr}/G$ is the length of frozen bits in one sub-block. In the proposed PC-HIM framework, in one sub-block, one position (antenna) is selected from $\mathcal{N}_t$ available antennas by utilizing the corresponding n_{fr} frozen bits. The expression of n_{fr} can be written as:

$$n_{fr} = \mathcal{N}_{fr}/G = \left\lfloor \log_2 \binom{\mathcal{N}_{fr}}{1} \right\rfloor. \tag{15}$$

Consider the scenario illustrated in Fig.4, where for a given sub-block g, the sequence following IM is $[0, \times, 1, \times]$ (as highlighted in the column of Fig.4). This sequence need to be modulated by a frozen bit set $\mathbf{F}_{v,g}$ with two frozen bits $[0, 1]$ (as highlighted in the column of Fig.4). The number of available spatial positions (antennas) $\mathcal{N}_t$ for SM is four. In the proposed scheme, all symbols within a single sub-block utilize the same set of frozen bits to designate the activation status of spatial positions. Utilizing BPSK, the symbol sequence $\mathbf{S}_g$ can be written as $[+1, \times, -1, \times]$. According to $\mathbf{F}_{v,g}$ and Table 2, the first symbol +1 is modulated to the second position, resulting in a column vector $[0, +1, 0, 0]^T$. Additionally, all four sub-carriers in the sub-block are modulated using the same set of frozen bits $\mathbf{F}_{v,g}$, aligning all sub-carriers in one OFDM-IM sub-block to the second spatial position as indicated by the highlighted row in Fig. 4.

TABLE 2. **A Look-Up Table of Antenna Selection for n_{fr} = 2, $\mathcal{N}_t$ = 4.**

Frozen Bits	Antenna Number
$[0, 0]$	1
$[0, 1]$	2
$[1, 0]$	3
$[1, 1]$	4

By concatenating all G sub-blocks, a matrix $\mathbf{B}_v$ of dimensions $\mathcal{N}_t \times \mathcal{N}_\ell$ is constructed, where $\mathcal{N}_\ell$ denotes the length of the IFFT operation. Each row vector $\mathbf{B}_v^{n_t}$ within this matrix

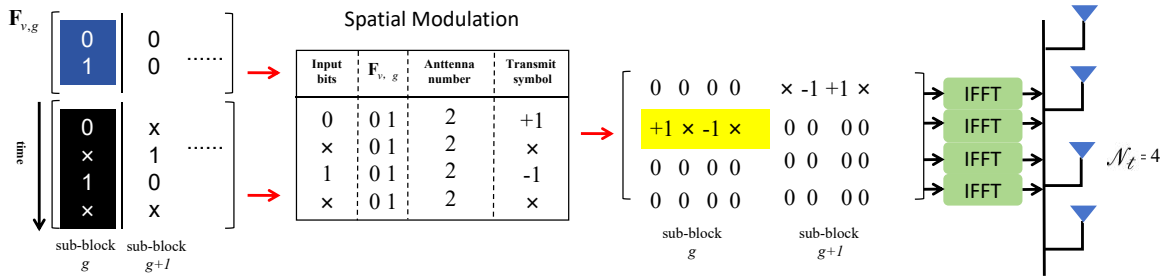

FIGURE 4. **The system model of the SM procedure of the proposed PC-HIM scheme**

contains the data to be transmitted across all sub-carriers via antenna n_t, where $n_t \in \{1, 2, ..., \mathcal{N}_t\}$. Subsequently, these row vectors are subjected to IFFT operations, resulting in the following transformations:

$$\mathbf{b}_v^{n_t} = \text{IFFT}(\mathbf{B}_v^{n_t}), \tag{16}$$

where $\mathbf{b}_v^{n_t} = (\mathbf{b}_v^{n_t}[1], \mathbf{b}_v^{n_t}[2], ..., \mathbf{b}_v^{n_t}[\mathcal{N}_f])$ with components:

$$\mathbf{b}_v^{n_t}[\rho] = \frac{1}{\mathcal{N}_f} \sum_{k=1}^{\mathcal{N}_f} \mathbf{B}_v^{n_t}[k] e^{j2\pi k\rho/\mathcal{N}_f}. \tag{17}$$

Unlike the previous existing polar-coded PAPR reduction schemes, the proposed PC-HIM framework is a MIMO-based PAPR reduction scheme. Therefore, the PAPR of the v^{th} candidate is defined as the maximum PAPR among all $\mathcal{N}_t$ row vectors $\mathbf{b}_v^{n_t}$, which is written as:

$$PAPR_{\text{mimo},v} = \max[PAPR_v^1, PAPR_v^2, ..., PAPR_v^{\mathcal{N}_t}], \tag{18}$$

where $PAPR_v^{n_t}$ is the $n_t{}^{th}$ PAPR for the v^{th} candidate, which is defined as [13]:

$$PAPR_v^{n_t} = \text{PAPR}\{\mathbf{b}_v^{n_t}\} \triangleq \frac{\max\limits_{1\le p\le \mathcal{N}_f} |\mathbf{b}_v^{n_t}[\rho]|^2}{P_{\mathbf{b}_v^{n_t}}}, \tag{19}$$

where $P_{\mathbf{b}_v^{n_t}}$ denotes the average power of $\mathbf{b}_v^{n_t}$, which is calculated as:

$$P_{\mathbf{b}_v^{n_t}} = \frac{1}{\mathcal{N}_f} E[\mathbf{b}_v^{n_t} \mathbf{b}_v^{n_t,H}] = \frac{1}{\mathcal{N}_f} E[||\mathbf{b}_v^{n_t}||^2], \tag{20}$$

where $E[\ ]$ denotes the expected value and the superscript H denotes the Hermitian transpose.

Then, among all V PAPR candidates, the system selects one candidate with the minimum PAPR as:

$$\tilde{v} = \underset{0\le v\le V}{\text{argmin}}\{PAPR_{\text{mimo},v}\}, \tag{21}$$

for transmission.

To identify the candidate $\mathbf{b}_{\tilde{v}}$ with the lowest PAPR, the proposed PC-HIM scheme for PAPR reduction requires V parallel SM and $V\mathcal{N}_t$ IFFT operations. This approach might lead to higher complexity compared to conventional SLM-based PAPR reduction schemes. To address this, a simplified version of the PC-HIM scheme (LC-PC-HIM) is introduced, utilizing a single SM, V IFFT instead of V parallel SM and $V\mathcal{N}_t$ IFFT operations to reduce the computational complexity.

As illustrated in Fig.5. The LC-PC-HIM scheme generates V distinct frequency domain candidates $\mathbf{S}_v$, each with varying PAPR. Following this, V IFFT operations convert these frequency domain candidates into their corresponding time-domain signals, denoted as $\mathbf{b}_v$. Each of these own different PAPR, which is denoted as $PAPR_v$, for $1 \le v \le V$. The system then selects the candidate with the lowest PAPR for transmission. This process can be expressed as follows:

$$\tilde{v} = \underset{0\le v\le V}{\text{argmin}}\{\text{PAPR}\{\mathbf{b}_v\}\}, \tag{22}$$

Following the candidate selection process, a SM operation based on $\mathbf{F}_{\tilde{v}}$ is applied to the selected transmission sequence $\mathbf{b}_{\tilde{v}}$. Consequently, $\mathbf{b}_{\tilde{v}}$ is distributed across $\mathcal{N}_t$ antennas based on the $\tilde{v}^{\text{th}}$ frozen bit set. With the LC-PC-HIM scheme, V IFFT operations are required, having the same complexity as that of conventional SLM based PAPR reduction schemes. Additionally, the PAPR of the v^{th} candidate is defined as the maximum PAPR among all $\mathcal{N}_t$ row vectors $\mathbf{b}_v^{n_t}$. This calculation is shown as:

$$PAPR_{\text{mimo},\tilde{v}} = \max[PAPR_{\tilde{v}}^1, PAPR_{\tilde{v}}^2, ..., PAPR_{\tilde{v}}^{\mathcal{N}_t}]. \tag{23}$$

It is important to highlight that in the proposed transmission scheme, the active antenna index for the g^{th} sub-block, denoted as $\tilde{n_t}_{,g}$, remains consistent within a single OFDM-IM sub-block g, where $1 \le \tilde{n_t}_{,g} \le \mathcal{N}_t$. This consistency ensures uniformity in the transmission process across the specified sub-block, which provides a good base for the following frozen bit set detection.

Upon concatenating all G sub-blocks, the resulting $\mathcal{N}_t \times \mathcal{N}_f$ output vectors, post OFDM-IM modulation, are simultaneously transmitted from the $\mathcal{N}_t$ antennas across the MIMO channel, denoted as $\mathbf{H}(\tau, t)$. This paper assumes a Rayleigh fading channel model, characteristic of a rich scattering environment typical of non-line-of-sight (NLOS) applications [42].

For all probabilistic based PAPR reduction schemes (SLM or PTS), side information must be transmitted. The side information representing the employed frozen bit set $\mathbf{F}_{\tilde{v}}$ must also be transmitted as extra bits. The conventional probabilistic based PAPR reduction schemes transmit at least

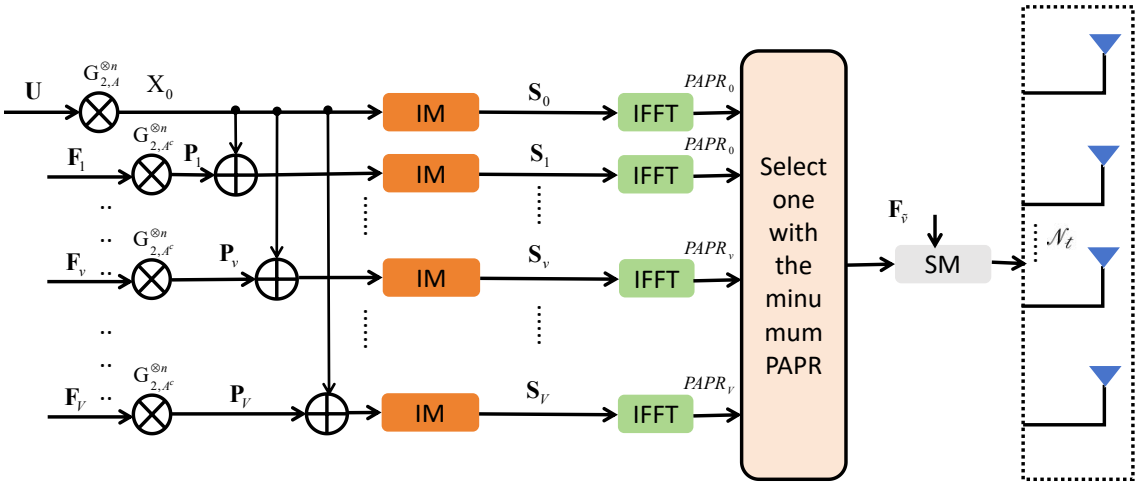

FIGURE 5. **The diagram of the proposed LC-PC-HIM transmitting framework**

$\log_2 V$ extra bits which negatively impact spectral efficiency and error performance. To avoid side information transmission, the proposed PAPR reduction scheme presents an side information-free receiving scheme that utilizes the transmitter structure and frozen bit sets in order to achieve impressive error performance without reducing spectral efficiency.

B. The Receiver

At the receiver, the received matrix $\mathbf{R}(t) = \mathbf{H}(\tau, t) \otimes \mathbf{S}(t) + \mathbf{W}(t)$ is processed, where $\mathbf{S}(t)$ represents the time-domain matrix encompassing all OFDM-IM symbols transmitted from each antenna, and $\mathbf{W}(t)$ denotes the matrix of additive white Gaussian noise (AWGN). The symbol $\otimes$ indicates time convolution. This received matrix is subsequently demodulated using $\mathcal{N}_r$ OFDM-IM demodulators. Considering a discrete-time representation for analysis, the output from these demodulators is formatted into a matrix $\mathbf{R}$ of size $\mathcal{N}_r \times \mathcal{N}_\ell$. Each column of $\mathbf{R}$ corresponds to the received data across the $\mathcal{N}_\ell$ OFDM-IM sub-carriers from each of the $\mathcal{N}_r$ receive antennas.

Subsequently, the received $\mathcal{N}_\ell$ OFDM-IM sequence undergoes equalization, which involves multiplication by the Hermitian conjugate of the channel's frequency response matrix, which is assumed to be known at the receiver [43]. The resulting equalized vector, denoted as $\mathbf{y}$, is expressed as follows:

$$\mathbf{y} = \mathbf{h}^H \mathbf{r}, \tag{24}$$

where $\mathbf{h}$ is the $\mathcal{N}_r \times \mathcal{N}_t$ discrete time-invariant frequency response channel matrix. and $\mathbf{r}$ is the corresponding demodulated OFDM-IM sequence of size $\mathcal{N}_r \times \mathcal{N}_\ell$.

Following equalization, the side information free receiving task involves detecting the index of the activated transmit antenna for each sub-carrier. Initially, the $\mathcal{N}_\ell$-length received OFDM-IM sequence is divided into G sub-blocks, each represented as $\mathbf{y}_g$, where $1 \leq g \leq G$. In the presence of AWGN, the estimated active antenna number, denoted as $\hat{\mathscr{A}nt}$, for each sub-block g is determined by:

$$\hat{\mathscr{A}nt} = \underset{\forall n_t}{\text{argmax}} \left(\sum_{\eta=1}^{n_t} |\mathbf{y}_g[\eta]|^2 \right), \quad n_t = 1, ..., \mathcal{N}_t. \tag{25}$$

Upon processing all G sub-blocks, the estimated frozen bits, denoted as $\hat{F}_{tmp}$, are de-mapped in accordance with the mappings specified in Table 2 by utilizing the estimated $\hat{\mathscr{A}nt}$. Given the constrained size of the random frozen bit sets, a valid index $\hat{v}$ for the frozen bits can be estimated using the maximum likelihood (ML) methodology:

$$\hat{v} = \underset{\forall v}{\text{argmin}} \left(\sum_{q=1}^{\mathcal{N}_{fr}} |F_v[q] - \hat{F}_{tmp}[q]| \right). \tag{26}$$

Following the estimation of the frozen bits, a vector $\mathbf{y1}$ of dimensions $1 \times \mathcal{N}_\ell$ is re-constructed, making use of the estimated combinations of activated antennas and frozen bits. Subsequent to this step, a frequency IM demodulation is performed. This demodulation considers the *a posteriori* probabilities of the frequency domain signals, discerning between non-zero and zero values [2]. Specifically, for the g^{th} sub-block, frequency IM demodulators calculate the probability of active status for each index η, where $\eta = 1, 2, ..., n$, as follows:

$$\lambda_g[\eta] = \ln \frac{\sum_{\chi=1}^{M} Pr(\mathbf{S}_g[\eta] = \Theta_\chi | \mathbf{y1}_g[\eta])}{Pr(\mathbf{S}_g[\eta] = 0 | \mathbf{y1}_g[\eta])}, \tag{27}$$

where Θ_χ is the element of a M-array constellation.

The lager the value of $\lambda_g[\eta]$, the higher the probability that the corresponding η is an active sub-carrier. Using Bayes

This article has been accepted for publication in IEEE Open Journal of the Communications Society. This is the author's version which has not been fully edited and content may change prior to final publication. Citation information: DOI 10.1109/OJCOMS.2024.3427628

formula, (27) can be expressed as:

$$\lambda_g[\eta] = \ln(k) - \ln(n-k) + \frac{|\mathbf{y1}_g[\eta]|^2}{\sigma_k^2} + \ln((\sum_{\chi=1}^{\mathrm{M}} \exp(-\frac{1}{\sigma_k^2}|\mathbf{y1}_g[\eta] - \Theta_\chi|^2)), \quad (28)$$

where σ_k is the noise variance in the frequency domain.

Upon the successful detection of the indices of antennas and active sub-carriers, the initial log-likelihood ratios (LLRs) necessary for polar decoding can be recovered and obtained. Consequently, a SC decoding procedure [44] can be employed. This decoding procedure is described in details in [26], which illustrates the principles of index modulation-based polar decoding. The implementation of this decoding strategy facilitates the accurate recovery of the transmitted information.

It should be noted that the procedure for estimating the index of the frozen bit set, as described in (26), may contribute to increased computational complexity and latency at the receiver. This is due to the fact that $\hat{v}$ can only be determined after all $\hat{\mathscr{Ant}}$ values for the G sub-blocks, as defined in (25), have been estimated. Consequently, to address these concerns, the following part of this section introduces a flexible method belonging to the framework of LC-PC-HIM for estimating frozen bits, specifically designed to reduce both complexity and latency.

Given that the number of random frozen bit sets utilized for PAPR reduction is limited (V), it is unnecessary to compare all $\mathscr{N}_{fr}$ frozen bits to determine the corresponding index $\tilde{v}$ as initially described in (26). Consequently, the estimation process can be streamlined by simplifying (26) to (29). This simplification facilitates a trade-off between complexity and decoding performance.

$$\hat{v} = \underset{\forall v}{\operatorname{argmin}}(\sum_{q=1}^{\mathscr{N}_{p,fr}} |F_v[q] - \hat{F}_{tmp}[q]|), \quad (29)$$

where $\mathscr{N}_{p,fr}$ is the length of bits that are utilized for selecting the index $\tilde{v}$, and the processed bit length $1 \leq \mathscr{N}_{p,fr} \leq \mathscr{N}_{fr}$. Moreover, according to the estimated $\hat{v}$ utilizing partial frozen bits, the corresponding following active antennas $\hat{\mathscr{Ant}}$ can be directly determined without detecting the rest of the received sequence using (25).

Here, we investigate the impact of the processed bit length, $\mathscr{N}_{p,fr}$, on the detection error rate of frozen bit sets (FSER). It is straightforward that shorter processed bit length may degrade the error performance by mis-detecting the selected frozen bit set easier. As illustrated in Fig.6, 16 different random frozen bit sets, each 64 bits long, are evaluated across various signal to noise ratio (SNR) scenarios. The FSER is evaluated for varying processed bit lengths, demonstrating that the estimation method for frozen bits is highly accurate. It can be seen from Fig.6 that when all 64 bits (even 48 bits) are compared, all selected frozen bit sets can be correctly detected. Additionally, it is observed that the required length of processed bits can be significantly reduced as the SNR increases. For instance, at an SNR of 7 dB, processing only 24 bits is sufficient to accurately determine the selected frozen bit set with $\tilde{v}$, which complexity is 37.5% of the original detecting method of PC-HIM scheme. Based on these findings, the potential for developing an adaptive detection method will be explored in future research.

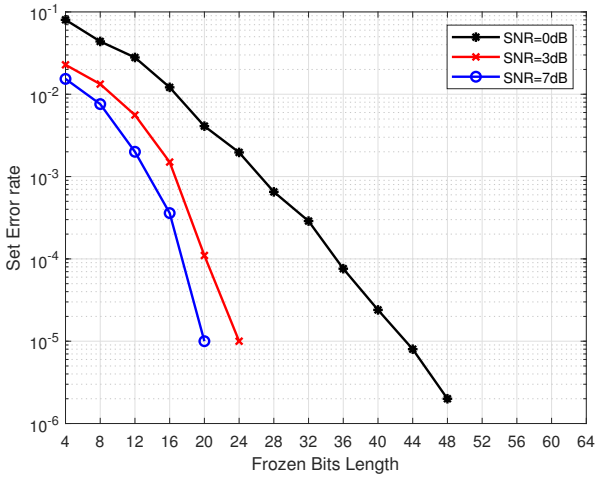

FIGURE 6. Frozen bit sets detection error rate (FSER) for the proposed receiver with variable processed bit length

The results presented in Fig.6 suggest that when the Hamming distance among the processed $\mathscr{N}_{p,fr}$ bits among different set is larger, the frozen bit sets are more easily distinguishable. This observation indicates a potential approach to creating multiple frozen bit sets with lower FSER, which in turn can help the detection system reduce computational complexity.

Therefore, to achieve a lower FSER with shorter processed frozen bits, this paper introduces a scheme for constructing frozen bit sets based on the Hadamard matrix. Hadamard codes, also known as Walsh sequences or first-order Reed–Muller codes up to interleaving [45], are widely used in communication systems for synchronization and bandwidth spreading. Hadamard sequences exhibit several key characteristics valuable for coding and communication. The Hamming distance for a Hadamard code of length $\mathscr{N}_{\mathscr{H}}$ ranges from $\mathscr{N}_{\mathscr{H}}/2$ to $\mathscr{N}_{\mathscr{H}}$ [46]. The maximum Hamming distance is achieved when two sequences are completely distinct, while the minimum occurs when half of the elements differ. Additionally, owing to the orthogonality of Hadamard matrices, the Hamming distance between any two distinct rows or columns is consistently half the matrix order. This attribute is particularly useful in communication systems and coding applications, where stable Hamming distances can enhance signal differentiation and improve error correction capabilities.

The generation of Hadamard matrix and Hadamard codes can begin with a 1×1 Hadamard matrix $\mathbf{Hd} = [+1]$. An

$\mathcal{N}_{\mathscr{H}} \times \mathcal{N}_{\mathscr{H}}$ Hadamard matrix $\mathbf{Hd}_{\mathcal{N}_{\mathscr{H}}}$ over $[+1, -1]$ can be constructed recursively as

$$\mathbf{Hd}_{\mathcal{N}_{\mathscr{H}}} = \begin{bmatrix} +\mathbf{Hd}_{\mathcal{N}_{\mathscr{H}}/2} & +\mathbf{Hd}_{\mathcal{N}_{\mathscr{H}}/2} \\ +\mathbf{Hd}_{\mathcal{N}_{\mathscr{H}}/2} & -\mathbf{Hd}_{\mathcal{N}_{\mathscr{H}}/2} \end{bmatrix}. \tag{30}$$

The set of Hadamard codewords, denoted as $\mathbf{Hd}$, is derived from the columns of $\pm\mathbf{Hd}_{\mathcal{N}_{\mathscr{H}}}$. Here, the codewords of the Hadamard matrix, $\mathbf{Hd}_{\mathcal{N}_{\mathscr{H}}}$, are represented by $\mathbf{hd}_{\mathcal{N}_{\mathscr{H}}}$, which can serve as frozen bits when -1 is replaced with 0. Given that the proposed PAPR reduction scheme requires a frozen bit length of $\mathcal{N}_{fr}$, the Hadamard matrix order $\mathcal{N}_{\mathscr{H}}$ is equivalent to $\mathcal{N}_{fr}$.

After obtaining the frozen bit set matrix $\mathbf{Hd}_{\mathcal{N}_{fr}}$, to decrease the length of processed bits, $\mathcal{N}_{p,fr}$, for V candidate sequences, it is essential to select the V frozen bits with the greatest Hamming distance for the first $\mathcal{N}_{p,fr}$ bits from the available $\mathcal{N}_{fr}$ generated Hadamard frozen bit codewords. This selection process can be performed recursively by comparing the Hamming distance among all available codewords, ensuring that the chosen frozen bits yield maximum differentiation among the candidate sequences. The corresponding frozen bits selection algorithm is given in Algorithm.1.

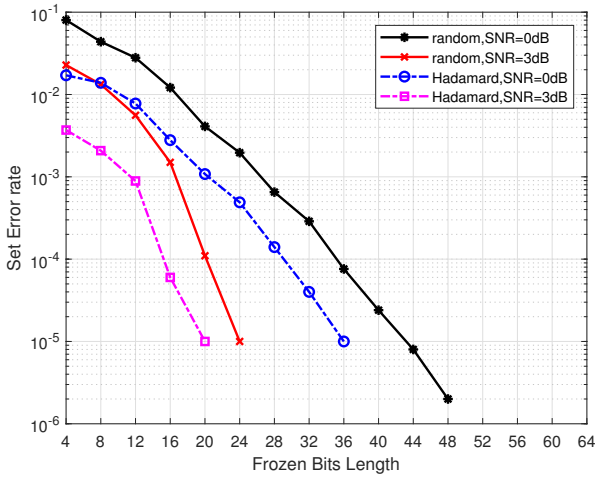

FIGURE 7. FSER comparison for the proposed receiver using different frozen bit sets selection method

The utilization of Algorithm.1 significantly enhances the system's ability to obtain an effective set of frozen bits, which in turn reduces the FSER. A comparative analysis of the FSER performance for the proposed receiver, employing various frozen bit selection schemes, is depicted in Fig.7. As demonstrated, the integration of the Hadamard sequence with frozen bit sets construction Algorithm.1 results in a substantial decrease in the FSER when SNRs are equivalent, thereby achieving higher detection accuracy and a reduced error rate at the receiver. It is important to note that the construction of the frozen bit sets can be executed offline, reducing potential burdens on overall computational complexity and latency.

Algorithm 1 Frozen Bits Selection Algorithm From An Order $\mathcal{N}_{\mathscr{H}}$ Hadamard Matrix

Input: The order of the Hadamard matrix, denoted as $\mathcal{N}_{\mathscr{H}}$
Output: V selected frozen bit sequences $\mathbf{F}_v$ with length $\mathcal{N}_{fr}$
Steps:
Generate a $\mathcal{N}_{\mathscr{H}}$-order Hadamard matrix, $\mathbf{Hd}_{\mathcal{N}_{\mathscr{H}}}$ according to (30)
Extract the first $\mathcal{N}_{fr}$ columns from $\mathbf{Hd}_{\mathcal{N}_{\mathscr{H}}}$ to form a sub-matrix, $\mathbf{Hd}_{\mathcal{N}_{\mathscr{H}},\mathcal{N}_{fr}}$
Generate an all zero distance matrix `dis` with size $\mathcal{N}_{\mathscr{H}} \times \mathcal{N}_{\mathscr{H}}$
for each pair (i, j), $i < j$, where $i, j \in [0, 1, \ldots, \mathcal{N}_{\mathscr{H}} - 1]$ **do**
    Compute the Hamming distance between row i and row j in the sub-matrix $\mathbf{Hd}_{\mathcal{N}_{\mathscr{H}},\mathcal{N}_{fr}}$
    Store the Hamming distance in `dis`
Initialize `comb_id`, containing all combinations of choosing V frozen bit sets out of $\mathcal{N}_{\mathscr{H}}$ available rows
Initialize an empty list `min_dis`
for each combination `ids` in `comb_id` **do**
    Initialize `min_dis` to infinity
    for each pair (i, j) within `ids` **do**
        Update `min_dis` to the minimum Hamming distance between rows in `dis`
    Append `(ids, min_dis)` to `min_dis`
Find the combination `max_dis_comb` in `min_dis` with the largest minimum Hamming distance
Get the V rows corresponding to `max_dis_comb`
Replace the -1 in the selected V rows to 0
Return the selected V frozen bit sets $\mathbf{F}_v$, $(v = 1, 2, ..., V)$

The proposed (LC-)PC-HIM PAPR reduction scheme can be summarized in Algorithm.2, where the selected frozen bit set $\tilde{v}$ can be generated from both PC-HIM and LC-PC-HIM schemes. The corresponding $\hat{v}$ selection method is given in Algorithm.3, where the estimated $\hat{v}$ can be selected for both PC-HIM and LC-PC-HIM schemes.

C. Complexity Analysis

In this subsection, we perform a complexity analysis of existing polar code-based PAPR reduction techniques by evaluating the computational demands at both the transmitter and receiver ends.

The complexity of a polar encoding process has been established as $\mathcal{O}(\mathcal{N}_p \log \mathcal{N}_p)$ [35]. In the novel polar-coded PAPR reduction scheme [27], the insertion of PAPR reduction bits is equivalent to encoding at a higher code rate, which also demands a complexity of $\mathcal{O}(\mathcal{N}_p \log \mathcal{N}_p)$. Additionally, the novel polar-coded PAPR reduction scheme [35] incorporates an IFFT operation, maintaining the same complexity level $\mathcal{O}(\mathcal{N}_f \log \mathcal{N}_f)$. Consequently, the overall

Algorithm 2 The Proposed (LC-)PC-HIM PAPR Reduction Scheme

Input: Frozen bit length $\mathcal{N}_{fr}$, V alternative sequences, input data sequence $\mathbf{U}$, indicator `indicator`, the antenna number $\mathcal{N}_t$
Output:Selected frozen bit set index $\tilde{v}$
Generate V sets of frozen bit $\mathbf{F}_v$, where $1 \leq v \leq V$, utilizing $\mathcal{N}_{fr}$ order Hadamard matrix based on Algorithm.1.
Generate V different polar codewords $\mathbf{X}_v$ according to (13)
Utilizing IM to V polar codewords $\mathbf{X}_v$ to obtain V OFDM-IM symbol sequences $\mathbf{S}_v$
if `indicator` == 1 (PC-HIM) **then**
  for v=1 to V **do**
    Do SM operation on $\mathbf{S}_v$, and generate $\mathbf{B}_v^{n_t}$, $n_t = 1, 2, ..., \mathcal{N}_t$
    for n_t=1 to $\mathcal{N}_t$ **do**
      Generate $\mathcal{N}_t$ sequences $\mathbf{b}_v^{n_t}$ using IFFT operations
      Calculate $\mathcal{N}_t$ PAPR $PAPR_v^{n_t}$ for candidate $\mathbf{S}_v$ according to (19)
      Append $PAPR_v^{n_t}$ to `papr_tmp`, which can be written as `papr_tmp`=[$PAPR_v^1$, $PAPR_v^2$,...,$PAPR_v^{\mathcal{N}_t}$]
    Select the maximum PAPR $PAPR_{\text{mimo},v}$ from set `papr_tmp`, and append it to `papr_v`, which can be written as `papr_v`=[$PAPR_{\text{mimo},1}$, $PAPR_{\text{mimo},2}$,...,$PAPR_{\text{mimo},V}$]
  Find the sequence $\tilde{v}$ with the lowest PAPR from set `papr_v`
else if `indicator` == 0 (LC-PC-HIM) **then**
  for v=1 to V **do**
    Generate V candidate sequences $\mathbf{b}_v$ using IFFT operations
    Calculate V PAPR $PAPR_v$ for candidate $\mathbf{S}_v$, and append it to `papr_v`, which can be written as `papr_v`=[$PAPR_1$, $PAPR_2$,...,$PAPR_V$]
  Find the sequence $\tilde{v}$ with the lowest PAPR from set `papr_v`
  Do SM operation on $\mathbf{S}_{\tilde{v}}$, and generate $\mathbf{B}_v^{n_t}$, $n_t = 1, 2, ..., \mathcal{N}_t$
  for n_t=1 to $\mathcal{N}_t$ **do**
    Calculate $\mathcal{N}_t$ PAPR $PAPR_{\tilde{v}}^{n_t}$ for candidate $\mathbf{S}_{\tilde{v}}$ according to (19)
    Append $PAPR_{\tilde{v}}^{n_t}$ to `papr_tmp`, which can be written as `papr_tmp`=[$PAPR_{\tilde{v}}^1$, $PAPR_{\tilde{v}}^2$,...,$PAPR_{\tilde{v}}^{\mathcal{N}_t}$]
  Select the maximum PAPR $PAPR_{\text{mimo},\tilde{v}}$ from set `papr_tmp` as the final PAPR performance result of LC-PC-HIM for further evaluation.
Return the selected frozen bit set index $\tilde{v}$

Algorithm 3 The $\hat{v}$ Selection Method for (LC-)PC-HIM PAPR Reduction Scheme

Input: Available frozen bit sets $\mathbf{F}_v$, Frozen bit length $\mathcal{N}_{fr}$, $\mathcal{N}_{p,fr}$ for detection, input equalized sequence $\mathbf{y}$, indicator `indicator`
Output:Selected frozen bit set index $\hat{v}$
Divide the $\mathcal{N}_f$-length received sequence $\mathbf{y}$ into G sub-blocks $\mathbf{y}_g$
for g=1 to G **do**
  Obtain the estimated activated antenna $\hat{\mathscr{A}nt}$ according to (25)
  Obtain the estimated frozen bit $\hat{F}_{tmp,g}$ by demapping $\hat{\mathscr{A}nt}$
Combing all $\hat{F}_{tmp,g}$ to construct an estimated frozen bit sequence $\hat{F}_{tmp}$ through the SM mapping rules
if `indicator` == 1 (PC-HIM) **then**
  Obtain an legal $\hat{v}$ according to the ML methodology in (26)
else if `indicator` == 0 (LC-PC-HIM) **then**
  Obtain an legal $\hat{v}$ according to the ML methodology in (29) by utilizing a shorten version of $\mathbf{F}_v$
Return the selected frozen bit set index $\hat{v}$

complexity for transmission in this novel scheme remains $\mathcal{O}(\mathcal{N}_p \log \mathcal{N}_p)$. On the receiver side, as described in [35], conventional SC decoding is employed, also with a complexity of $\mathcal{O}(\mathcal{N}_p \log \mathcal{N}_p)$. In contrast, the polar-coded SLM PAPR reduction scheme combined with OFDM-IM [28] involves generating and implementing V polar encoding process and V IFFT operations, respectively, elevating the overall transmission complexity to $\mathcal{O}(V\mathcal{N}_p \log \mathcal{N}_p)$. At the receiver, V SC-list decodings [47] are performed with a list size L, increasing in a complexity of $\mathcal{O}(VL\mathcal{N}_p \log \mathcal{N}_p)$. This complicated step is necessary for determining the selected frozen bit set. Subsequent SC-based decoding is then carried out to recover the transmitted information, maintaining a complexity of $\mathcal{O}(\mathcal{N}_p \log \mathcal{N}_p)$. Hence, the overall receiving complexity for the polar-coded SLM PAPR reduction scheme is $\mathcal{O}((VL+1)\mathcal{N}_p \log \mathcal{N}_p)$. For the polar-coded PTS PAPR reduction scheme with OFDM-IM [29], assuming G_{pts} denotes the number of PTS blocks, the total transmission complexity is derived as $\mathcal{O}(G_{pts}^2 \mathcal{N}_p \log \mathcal{N}_p)$. This complexity results from G_{pts} IFFT operations and G_{pts}^2 polar encoding processes. Regarding the receiving complexity, it is similar to that of the polar-coded SLM scheme [28], resulting in $\mathcal{O}((G_{pts}^2 L+1)\mathcal{N}_p \log \mathcal{N}_p)$.

In the proposed PC-HIM scheme, V polar codes are generated, resulting in a complexity of $\mathcal{O}(V\mathcal{N}_p \log \mathcal{N}_p)$. This complexity escalates to $\mathcal{O}(\mathcal{N}_t V\mathcal{N}_p \log \mathcal{N}_p)$ due to the requirement of $\mathcal{N}_t V$ IFFT operations for transmission. However, by employing the LC-PC-HIM PAPR reduction scheme, this complexity can be mitigated to $\mathcal{O}(V\mathcal{N}_p \log \mathcal{N}_p)$, aligning it with the complexity reported in [28]. On the receiving side, based on the selection and comparison of $\mathcal{N}_{p,fr}$ frozen bits as

shown in (29), the complexity is concluded as $\mathcal{O}(V\mathcal{N}_p,_{fr})$. Subsequent to the selection of frozen bit sets, SC decoding is executed, introducing an additional complexity of $\mathcal{O}(\mathcal{N}_p \log \mathcal{N}_p)$. Consequently, the total receiving complexity of the PC-HIM PAPR reduction scheme is determined to be $\mathcal{O}(\mathcal{N}_p \log \mathcal{N}_p)$, which represents a substantial reduction compared to the complexities associated with the existing polar-coded PAPR reduction schemes in [28] and [29]. The complexities of all polar-coded PAPR reduction schemes, in terms of both transmitter and receiver, are summarized in Table.3. The table shows that the proposed LC-PC-HIM scheme has the same complexity as that of the scheme in [28] and the lowest receiving complexity. Nevertheless, as a probabilistic PAPR reduction scheme, generating V different candidates typically requires V IFFT operations, resulting in higher computational complexity. Therefore, reducing the complexity of the proposed PAPR reduction scheme remains an open issue for future research. Future work could draw insights from existing studies on conventional SLM schemes.

IV. Simulation Result

In this section, we first conduct a comparative analysis of PAPR reduction performance (evaluated by complementary cumulative distribution function, CCDF) across various polar-coded PAPR reduction schemes. CCDF is a value that describes the power distribution. It indicates the probability that the PAPR of a signal exceeds a certain threshold $PAPR_0$.

$$CCDF = Pr(PAPR \geq PAPR_0). \tag{31}$$

The comparison includes the original OFDM-IM, the proposed PC-HIM scheme, the low-complexity LC-PC-HIM scheme, polar-coded PTS (denoted as "Polar-PTS") scheme [29], the novel polar-coded PAPR reduction approach in [27] (denoted as "Polar-Novel"), the conventional SLM scheme in polar-coded OFDM-IM systems (denoted as "SLM"), and the polar-coded SLM scheme in [28] (denoted as "Polar-SLM"). During these simulations, phase rotation vectors are randomly chosen from the set $\{-1, 1\}$. Frozen bits are constructed following Algorithm 1, with polar codewords of length $\mathcal{N}_p = 128$. For polar-coded OFDM-IM based schemes, hard detection is employed for index bit detection [26] and SC is used for polar decoding. The number of sub-blocks in OFDM-IM is set to 32. Additionally, the influence of the number of frozen bit sets V on the proposed schemes is examined. Comparative results also include the performance of an OFDM-IM system without any PAPR reduction scheme (denoted as "Unmod").

Next, we analyze the BER performance of the proposed method by comparing it with existing polar-coded PAPR reduction schemes within OFDM-IM systems. Specifically, the BER performance of the proposed PC-HIM is examined against that of the Polar-SLM scheme [28] and an idealized version of PC-HIM that utilizes perfect side information reception (denoted as "ideal"). For this analysis, polar codes with a codeword length of $\mathcal{N}_p = 128$ and a code rate R of 0.5 are used. SC decoding is employed to evaluate the BER performance in frequency-selective channels.

A. PAPR Reduction Performance

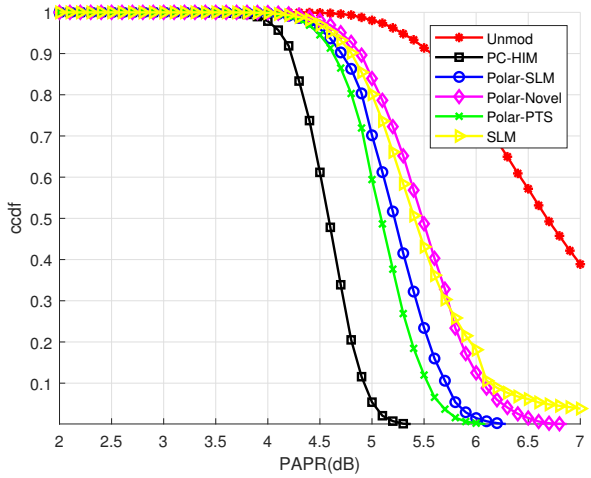

FIGURE 8. Comparison of CCDFs among different polar-coded based PAPR reduction schemes, with 16 candidates for $N_p = 128$.

The PAPR reduction performance comparison among the proposed PC-HIM scheme, Polar-SLM scheme, Polar-PTS scheme, SLM scheme, and Polar-Novel schemes is given in Fig.8. Each scheme employs 16 candidate sequences for fair comparison. Specifically, the Polar-PTS scheme is configured with 4 blocks, also yielding 16 candidates in total. The results demonstrate that all schemes can significantly enhance PAPR reduction performance. As shown in Fig.8, the Polar-Novel scheme, which utilizes redundant injected PAPR reduction bits, achieves notable PAPR reduction performance, which is similar to the conventional SLM scheme utilized in polar-coded OFDM-IM systems. However, due to the limited number of available PAPR reduction bits, the scheme detailed in [27] does not surpass other polar code-based PAPR reduction schemes in corresponding performance. The Polar-PTS scheme slightly outperforms the Polar-SLM due to its permutation operations. Despite the higher complexity at the transmitter, the proposed PC-HIM scheme delivers the most effective PAPR reduction among the compared polar-coded schemes, benefiting significantly from the integration of spatial modulation. Additionally, by adopting the LC-PC-HIM scheme, the proposed approach can also achieve enhanced PAPR reduction performance with complexities comparable to those of the Polar-PTS and Polar-SLM schemes, which is shown in the next part.

The PAPR reduction performance comparison among the proposed PC-HIM scheme, its low-complexity version (LC-PC-HIM), and the Polar-SLM schemes is presented in Fig.9. For a fair comparison, each scheme utilizes 16 candidate sequences. As shown in Fig.9, the LC-PC-HIM experiences a decrease in PAPR reduction performance compared to the standard PC-HIM framework, due to its significant

This article has been accepted for publication in IEEE Open Journal of the Communications Society. This is the author's version which has not been fully edited and content may change prior to final publication. Citation information: DOI 10.1109/OJCOMS.2024.3427628

TABLE 3. The Complexity Analysis Among Existing Polar Code-Based PAPR Reduction Schemes

Scheme	Transmitter	Complexity	Receiver	Complexity
Polar-Novel [27]	$\mathcal{O}(\mathcal{N}_p \log \mathcal{N}_p)$	Low	$\mathcal{O}(\mathcal{N}_p \log \mathcal{N}_p)$	Low
Polar-SLM [28]	$\mathcal{O}(V\mathcal{N}_p \log \mathcal{N}_p)$	Medium	$\mathcal{O}((VL+1)\mathcal{N}_p \log \mathcal{N}_p)$	High
Polar-PTS [29]	$\mathcal{O}(G_{pts}^2 \mathcal{N}_p \log \mathcal{N}_p)$	Medium	$\mathcal{O}((G_{pts}^2 L+1)\mathcal{N}_p \log \mathcal{N}_p)$	High
PC-HIM	$\mathcal{O}(\mathcal{N}_t V \mathcal{N}_p \log \mathcal{N}_p)$	High	$\mathcal{O}(\mathcal{N}_p \log \mathcal{N}_p)$	Low
LC-PC-HIM	$\mathcal{O}(V\mathcal{N}_p \log \mathcal{N}_p)$	Medium	$\mathcal{O}(\mathcal{N}_p \log \mathcal{N}_p)$	Low

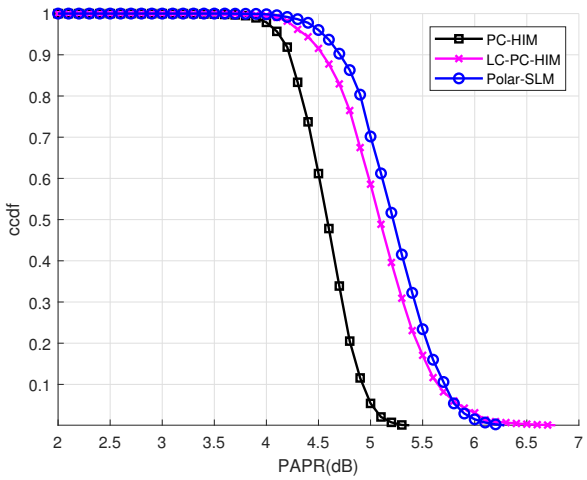

FIGURE 9. Comparison of CCDFs among PC-HIM Polar-SLM, and LC-PC-HIM schemes, with 16 candidates for $N_p = 128$.

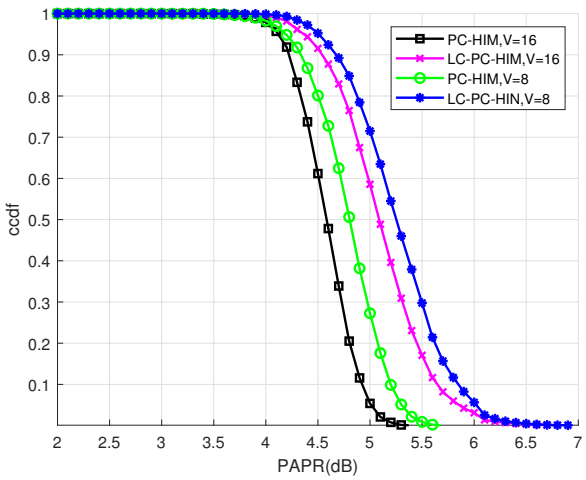

FIGURE 10. Comparison of CCDFs between PC-HIM and LC-PC-HIM schemes using variant V.

reduction in complexity. Notably, it has been illustrated in the last section that the complexity of LC-PC-HIM is only $1/\mathcal{N}_t$ of the conventional PC-HIM scheme, aligning it with the complexity of the Polar-SLM PAPR reduction scheme. However, with equivalent computational complexity, the LC-PC-HIM framework demonstrates marginally superior PAPR reduction performance compared to Polar-SLM scheme, as shown in Fig.9. Consequently, it can be concluded that the proposed LC-PC-HIM framework achieves enhanced PAPR reduction performance without an increase in system complexity.

The PAPR reduction performance comparison between the PC-HIM and its low-complexity version (LC-PC-HIM) across varying candidate numbers (V) is illustrated in Fig.9. The figure demonstrates that, despite doubling the number of candidates (V), the LC-PC-HIM achieves inferior PAPR reduction performance compared to the PC-HIM. Furthermore, an increase in V leads to improvements in PAPR reduction for both the LC-PC-HIM and PC-HIM schemes. However, the extent of performance enhancement in LC-PC-HIM is not as pronounced as that observed in PC-HIM, indicating a diminishing return on performance gains with increased candidate numbers in the corresponding low-complexity scheme.

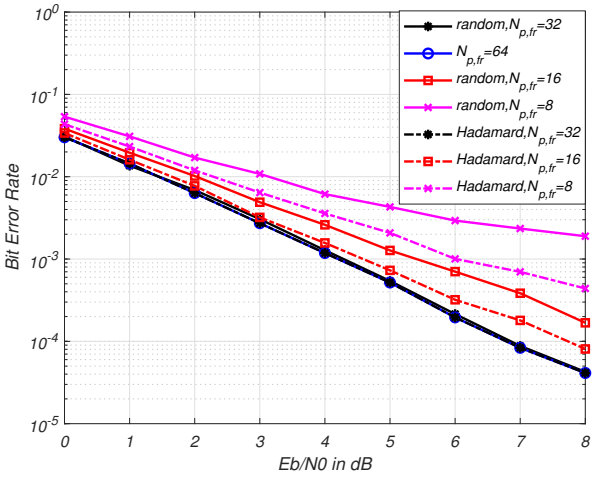

FIGURE 11. Comparison of BER among the proposed PAPR reduction utilizing different detection method and frozen bits length $N_{p,fr}$.

B. BER Performance

In our analysis of BER performance for the proposed side information-free PAPR reduction scheme, we first examined the impact of the length of detected frozen bits ($\mathcal{N}_{p,fr}$) on the overall BER performance in polar-coded OFDM systems. As illustrated in Fig.11, when frozen bit sets are constructed by random frozen bits, the BER performance generally degrades with a reduction in $\mathcal{N}_{p,fr}$, compared to the scenario

where all frozen bits are detected ($\mathcal{N}_{p,fr}$=64). However, an exception occurs when $\mathcal{N}_{p,fr}$ is halved, which means that a reduction in $\mathcal{N}_{p,fr}$ may not affect the corresponding error performance. Notably, when the detected frozen bit length is reduced to 1/4 of the original, a significant BER degradation is observed at BER=10^{-3}, with an SNR degradation of approximately 1.5 dB. This reduction in detection complexity, despite leading to poorer BER performance, represents a trade-off between complexity and error rate efficiency.

Additionally, Fig.11 explores the impact of using the proposed frozen bit sets construction method in Algorithm.1 on the overall BER performance in polar-coded OFDM systems. The results clearly demonstrate that employing Hadamard sequences alongside the frozen bit set construction method outlined in Algorithm 1 significantly enhances the corresponding error performance. Notably, compared to configurations using randomly selected frozen bit sets, employing the proposed frozen bit sets construction method results in an approximate 1 dB gain at a BER of 2×10^{-3} when $\mathcal{N}_{p,fr}$=16. Moreover, when $\mathcal{N}_{p,fr}$=8, the gain in SNR increases to 4 dB at a BER of 2×10^{-3}. These findings show the effectiveness of the proposed frozen bit set construction method in this paper.

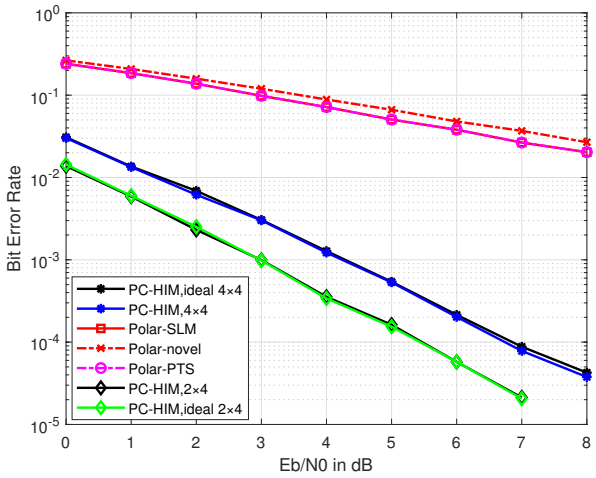

FIGURE 12. Comparison of the BER performance among different PAPR reduction schemes.

Subsequently, the BER performance of the proposed PC-HIM PAPR reduction scheme is compared with existing polar code-based PAPR reduction schemes in Fig.12. Additionally, to serve as a performance benchmark, the proposed scheme implemented with perfect side information reception is also evaluated (denoted as "PC-HIM, ideal"). As illustrated in Fig.12, by utilizing the side information-free receiving approach, the proposed PC-HIM achieves error performance nearly equivalent to that of the ideal case, where all selected frozen bit sets are correctly detected. Among the evaluated schemes, the "Polar-Novel" scheme achieves the poorest BER performance, primarily due to an increased code rate. Both the Polar-SLM and Polar-PTS exhibit identical error performance, as they utilize the same decoding and detecting methodology. Moreover, by integrating spatial modulation, the proposed PC-HIM significantly outperforms other polar code-based PAPR reduction schemes in terms of BER improvement. Also, in Fig.12, the error performance with different antennas configuration is also investigated. It is shown that compared with the 4×4 antenna configuration, the 2×4 antenna configuration is more effective in terms of BER performance.

V. Conclusion

In this paper, we propose a polar-coded PAPR reduction scheme for OFDM-IM systems, relying on hybrid index modulation. The proposed PC-HIM framework utilizes random frozen bit sets and spatial modulation to effectively reduce high PAPR in OFDM-IM systems. At the receiver, the PC-HIM detects the selected frozen bit set through activated antennas. This detection performance can be further enhanced with a novel construction method based on Hadamard sequence. Also, in this paper, to further address the complexity issues associated with the PC-HIM scheme, a low-complexity framework, termed LC-PC-HIM, is proposed. This framework implements candidate selection before spatial modulation, significantly reducing transmission complexity. Additionally, the LC-PC-HIM on the receiving side employs a shortened version of frozen bits for detecting the selected set, further decreasing receiving complexity. Simulation results demonstrate that both the PC-HIM and LC-PC-HIM schemes achieve superior PAPR reduction performance compared to existing polar code-based PAPR reduction schemes. Moreover, due to the incorporation of hybrid index modulation, the proposed scheme improves error performance over these existing methods. Also, as a side information-free framework, simulation results show that the proposed (LC-)PC-HIM scheme can achieve error performance comparable to that of an ideal receiver equipped with perfect side information.

REFERENCES

[1] W. Shieh, "Ofdm for flexible high-speed optical networks," *Journal of lightwave technology*, vol. 29, no. 10, pp. 1560–1577, 2011.

[2] E. Başar, Ü. Aygölü, E. Panayırcı, and H. V. Poor, "Orthogonal frequency division multiplexing with index modulation," *IEEE Transactions on Signal Processing*, vol. 61, no. 22, pp. 5536–5549, 2013.

[3] E. Basar, M. Wen, R. Mesleh, M. Di Renzo, Y. Xiao, and H. Haas, "Index modulation techniques for next-generation wireless networks," *IEEE access*, vol. 5, pp. 16 693–16 746, 2017.

[4] P. Yang, Y. Xiao, M. Xiao, and S. Li, "6g wireless communications: Vision and potential techniques," *IEEE network*, vol. 33, no. 4, pp. 70–75, 2019.

[5] X. Cheng, M. Zhang, M. Wen, and L. Yang, "Index modulation for 5g: Striving to do more with less," *IEEE Wireless Communications*, vol. 25, no. 2, pp. 126–132, 2018.

[6] P. Yang, Y. Xiao, Y. L. Guan, M. Di Renzo, S. Li, and L. Hanzo, "Multi-domain index modulation for vehicular communications: A survey," *IEEE Vehicular Technology Magazine*, 2018.

[7] H. Zhang, L.-L. Yang, and L. Hanzo, "Ldpc-coded index-modulation aided ofdm for in-vehicle power line communications," in *2016 IEEE 83rd Vehicular Technology Conference (VTC Spring)*. IEEE, 2016, pp. 1–5.

[8] Y. Cui and X. Fang, "Performance analysis of massive spatial modulation mimo in high-speed railway," *IEEE Transactions on Vehicular Technology*, vol. 65, no. 11, pp. 8925–8932, 2016.

[9] Q. Li, M. Wen, and M. Di Renzo, "Single-rf mimo: From spatial modulation to metasurface-based modulation," *IEEE Wireless Communications*, vol. 28, no. 4, pp. 88–95, 2021.

[10] Q. Li, M. Wen, E. Basar, H. V. Poor, and F. Chen, "Spatial modulation-aided cooperative noma: Performance analysis and comparative study," *IEEE Journal of Selected Topics in Signal Processing*, vol. 13, no. 3, pp. 715–728, 2019.

[11] H. Zhao, D. He, Z. Kang, and H. Wang, "Orthogonal time frequency space (otfs) with dual-mode index modulation," *IEEE Wireless Communications Letters*, vol. 10, no. 5, pp. 991–995, 2021.

[12] Y. Wang, W. Chen, and C. Tellambura, "A papr reduction method based on artificial bee colony algorithm for ofdm signals," *IEEE transactions on wireless communications*, vol. 9, no. 10, pp. 2994–2999, 2010.

[13] S.-y. Zhang and B. Shahrrava, "A selected mapping technique using interleavers for papr reduction in ofdm systems," *Wireless Personal Communications*, vol. 99, no. 1, pp. 329–338, 2018.

[14] M. Xiao, S. Mumtaz, Y. Huang, L. Dai, Y. Li, M. Matthaiou, G. K. Karagiannidis, E. Björnson, K. Yang, I. Chih-Lin *et al.*, "Millimeter wave communications for future mobile networks," *IEEE Journal on Selected Areas in Communications*, vol. 35, no. 9, pp. 1909–1935, 2017.

[15] J. Joung, C. K. Ho, K. Adachi, and S. Sun, "A survey on power-amplifier-centric techniques for spectrum-and energy-efficient wireless communications," *IEEE Communications Surveys & Tutorials*, vol. 17, no. 1, pp. 315–333, 2014.

[16] S. H. Han and J. H. Lee, "An overview of peak-to-average power ratio reduction techniques for multicarrier transmission," *IEEE wireless communications*, vol. 12, no. 2, pp. 56–65, 2005.

[17] L. Wang and C. Tellambura, "An overview of peak-to-average power ratio reduction techniques for ofdm systems," in *2006 IEEE International Symposium on Signal Processing and Information Technology*. IEEE, 2006, pp. 840–845.

[18] B. Robert, F. Robert, and B. Johannes, "Reducing the peak-to-average power ratio of multicarrier modulation by selected mapping," *Electronics letters*, vol. 32, no. 22, pp. 2056–2057, 1996.

[19] S. H. Müller and J. B. Huber, "Ofdm with reduced peak-to-average power ratio by optimum combination of partial transmit sequences," *Electronics letters*, vol. 33, no. 5, pp. 368–369, 1997.

[20] J. Ji, G. Ren, and H. Zhang, "A semi-blind slm scheme for papr reduction in ofdm systems with low-complexity transceiver," *IEEE Transactions on Vehicular Technology*, vol. 64, no. 6, pp. 2698–2703, 2014.

[21] H.-S. Joo, S.-J. Heo, H.-B. Jeon, J.-S. No, and D.-J. Shin, "A new blind slm scheme with low decoding complexity for ofdm systems," *IEEE transactions on broadcasting*, vol. 58, no. 4, pp. 669–676, 2012.

[22] K.-H. Kim, "Papr reduction in ofdm-im using multilevel dither signals," *IEEE Communications Letters*, vol. 23, no. 2, pp. 258–261, 2019.

[23] J. Zheng and H. Lv, "Peak-to-average power ratio reduction in ofdm index modulation through convex programming," *IEEE Communications Letters*, vol. 21, no. 7, pp. 1505–1508, 2017.

[24] S.-Y. Zhang and H. Zheng, "A hybrid papr reduction scheme in ofdm-im using phase rotation factors and dither signals on partial subcarriers," *Entropy*, vol. 24, no. 10, p. 1335, 2022.

[25] V. Bioglio, C. Condo, and I. Land, "Design of polar codes in 5g new radio," *IEEE Communications Surveys & Tutorials*, vol. 23, no. 1, pp. 29–40, 2020.

[26] S.-Y. Zhang and B. Shahrrava, "Polar-coded ofdm with index modulation," *IEEE Access*, vol. 9, pp. 237–247, 2020.

[27] T. Matsumine and H. Ochiai, "A novel papr reduction scheme for polar-coded ofdm systems," *IEEE Communications Letters*, vol. 23, no. 12, pp. 2372–2375, 2019.

[28] S.-Y. Zhang and B. Shahrrava, "A slm scheme for papr reduction in polar coded ofdm-im systems without using side information," *IEEE Transactions on Broadcasting*, vol. 67, no. 2, pp. 463–472, 2020.

[29] S.-Y. Zhang, B. Shahrrava, Y.-X. Zhang, and Z.-H. Zhuo, "A permutated partial transmit sequence scheme for papr reduction in polar-coded ofdm-im systems," *IEEE Transactions on Vehicular Technology*, 2023.

[30] S.-C. Lim, N. Kim, and H. Park, "Polar coding-based selective mapping for papr reduction without redundant information transmission," *IEEE Communications Letters*, vol. 24, no. 8, pp. 1621–1625, 2020.

[31] X. Lu, Y. Shi, W. Li, J. Lei, and Z. Pan, "A joint physical layer encryption and papr reduction scheme based on polar codes and chaotic sequences in ofdm system," *IEEE Access*, vol. 7, pp. 73 036–73 045, 2019.

[32] C.-C. Huang, T.-C. Kao, C.-Y. Pai, and C.-Y. Chen, "A novel scheme for peak-to-average power ratio reduction using polar codes," in *2022 10th International Workshop on Signal Design and Its Applications in Communications (IWSDA)*. IEEE, 2022, pp. 1–5.

[33] R. Y. Mesleh, H. Haas, S. Sinanovic, C. W. Ahn, and S. Yun, "Spatial modulation," *IEEE Transactions on vehicular technology*, vol. 57, no. 4, pp. 2228–2241, 2008.

[34] N. Ishikawa, S. Sugiura, and L. Hanzo, "Subcarrier-index modulation aided ofdm-will it work?" *IEEE Access*, vol. 4, pp. 2580–2593, 2016.

[35] E. Arikan, "Channel polarization: A method for constructing capacity-achieving codes for symmetric binary-input memoryless channels," *IEEE Transactions on Information Theory*, vol. 55, no. 7, pp. 3051–3073, 2009.

[36] Z. B. K. Egilmez, L. Xiang, R. G. Maunder, and L. Hanzo, "The development, operation and performance of the 5g polar codes," *IEEE Communications Surveys & Tutorials*, vol. 22, no. 1, pp. 96–122, 2019.

[37] K. NIU, B.-L. WU, J.-J. DAI, S. YU, and Y.-F. YUAN, "Polar coded modulation for 6g system," *Journal of Beijing University of Posts and Telecommunications*, vol. 45, no. 6, p. 1, 2022.

[38] H. Vangala, E. Viterbo, and Y. Hong, "A comparative study of polar code constructions for the awgn channel," *arXiv preprint arXiv:1501.02473*, 2015.

[39] S.-Y. Zhang and B. Shahrrava, "A hybrid sphere decoding for short polar codes using variable step size," *Physical Communication*, vol. 49, p. 101466, 2021.

[40] ——, "Belief propagation polar decoding for wireless communication systems with noisy channel estimates," *Wireless Personal Communications*, vol. 123, no. 2, pp. 1365–1377, 2022.

[41] S.-y. Zhang and B. Shahrrava, "Enhanced bp decoding schemes of polar codes," *IET Communications*, vol. 15, no. 9, pp. 1133–1142, 2021.

[42] J. Jeganathan, A. Ghrayeb, L. Szczecinski, and A. Ceron, "Space shift keying modulation for mimo channels," *IEEE transactions on wireless communications*, vol. 8, no. 7, pp. 3692–3703, 2009.

[43] I. Barhumi, G. Leus, and M. Moonen, "Optimal training design for mimo ofdm systems in mobile wireless channels," *IEEE Transactions on signal processing*, vol. 51, no. 6, pp. 1615–1624, 2003.

[44] I. Tal and A. Vardy, "List decoding of polar codes," in *Information Theory Proceedings (ISIT), 2011 IEEE International Symposium on*. IEEE, 2011, pp. 1–5.

[45] F. J. MacWilliams and N. J. A. Sloane, *The theory of error-correcting codes*. Elsevier, 1977, vol. 16.

[46] L. Ping, W. Leung, and K. Y. Wu, "Low-rate turbo-hadamard codes," *IEEE Transactions on Information Theory*, vol. 49, no. 12, pp. 3213–3224, 2003.

[47] K. Niu and K. Chen, "Crc-aided decoding of polar codes," *IEEE communications letters*, vol. 16, no. 10, pp. 1668–1671, 2012.

Si-Yu Zhang(Member, IEEE) received his Ph.D degree in electrical and computer engineering from the University of Windsor, Ontario, Canada, in 2021. He is currently an associate professor in the School of Information and Communication Engineering, Beijing Information Science and Technology University (BISTU). His current research interests include beyond 5G techniques, OTFS and IM techniques, coding and information theory, especially the design of polar decoders for 5G wireless networks. He is a Member of the IEEE.

Xinwei Yue(Senior Member, IEEE) Xinwei Yue received the Ph.D. degree in communication and information system from Beihang University, Beijing, China, in 2018. Since December 2018, he has been an Associate Professor with the School of Information and Communication Engineering, Beijing Information Science and Technology University, Beijing. His research interests include B5G/6G networks, non-orthogonal multiple access, reconfigurable intelligent surface, cooperative communications, and physical layer security. He was the recipient of the Exemplary Reviewer of the IEEE Transactions on Communications and IEEE Communication Letters in 2019 and 2022. He is the Editor of the IEEE System Journal and KSII Transactions on Internet and Information Systems.

Behnam Shahrrava(Member, IEEE) received his Ph.D. degree in electrical engineering from the University of Waterloo, Ontario, Canada, in 1998. He is currently an associate professor in the Department of Electrical and Computer Engineering, University of Windsor, Ontario, Canada. His research interests are in the areas of advanced statistical and adaptive signal processing and their applications, primarily in wireless communications, multiuser detection, iterative decoding algorithms, and turbo receiver design. He is a Member of the IEEE.

Yuexia Zhang(Senior Member, IEEE) received her PhD from Beijing University of Posts and Telecommunications in 2008. She is now professor with the School of Information and Communication Engineering, Beijing Information Science and Technology University. Her current research interests include wireless communication technology, indoor positioning and internet of vehicles technology.

Gongpu Wang(Member, IEEE) eceived the B.Eng. degree in communication engineering from Anhui University, Hefei, China, in 2001, the M.Sc. degree from the Beijing University of Posts and Telecommunications, Beijing, China, in 2004, and the Ph.D. degree from the University of Alberta, Edmonton, AB, Canada, in 2011. From 2004 to 2007, he was an Assistant Professor with the School of Network Education, Beijing University of Posts and Telecommunications. He is currently a Full Professor with the School of Computer and Information Technology, Beijing Jiaotong University, Beijing, China. His research interests include wireless communication theory, signal processing technologies, and the Internet of Things.